

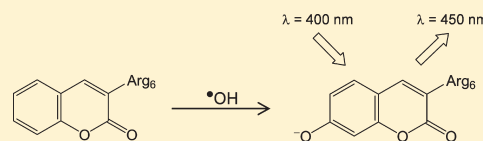
Use of a Coumarin-Labeled Hexa-Arginine Peptide as a Fluorescent Hydroxyl Radical Probe in a Nanoparticulate Plasmid DNA Condensate

Christopher C. Perry,[†] Vicky J. Tang,[‡] Katie M. Konigsfeld,[‡] Joseph A. Aguilera,[‡] and Jamie R. Milligan^{*,‡}

[†]Department of Biochemistry, Mortensen Hall, Loma Linda University, 11085 Campus Street, Loma Linda, California 92350, United States

[‡]Department of Radiology, University of California at San Diego, 9500 Gilman Drive, La Jolla, California 92093-0610, United States

ABSTRACT: Coumarin derivatives have found application as probes for the hydroxyl radical because one of the products of the reaction between them is a highly fluorescent umbelliferone. We have examined the interaction in aqueous solution between a cationic coumarin-labeled hexa-arginine peptide ligand and plasmid DNA, and compared after gamma irradiation the yields of products derived from both of them. At low ionic strengths, the ligand binds very tightly to the plasmid. Compared with the structurally similar 4-methylumbelliferone (phenolic $pK_a = 7.8$), the fluorescent product derived from gamma irradiation of the coumarin labeled cationic peptide is significantly more acidic ($pK_a = 6.1$), making it a very convenient probe for solutions of pH in the physiological range. The yield of this product is generally in excellent agreement over a wide range of conditions with that of the single strand break product produced by the reaction of the hydroxyl radical with the plasmid. Thus coumarin-labeled peptide ligands offer promise as hydroxyl radical probes for locations in close proximity to DNA.



INTRODUCTION

Ionizing radiation produces DNA damage in cells.¹ These chemical modifications are produced by two different routes: the direct effect (ionization of the DNA itself) and the indirect effect (ionization of the aqueous solvent medium to produce reactive intermediates that subsequently react with DNA). The principal species responsible for the indirect effect is the hydroxyl radical.² It is generally assumed that the reactions of the DNA radical species that result from these two routes are responsible for the formation of stable chemically modified products.^{3,4} These chemical modifications of the DNA are referred to as direct-type or indirect-type damage.^{5–7}

The contribution of the direct effect in dilute solution is very small, because the vast majority of the ionizations take place in the solvent. In the nuclei of cells, however, the high concentration of DNA⁸ leads to an increase in the efficiency of the direct effect over that in a dilute solution typical of a cell free experimental system. In addition, the high concentration in the nucleus of numerous other species that compete with the DNA for the hydroxyl radical decreases the efficiency of the indirect effect. The combination of these factors results in a situation where both the direct and the indirect effects make a significant contribution to the DNA damage produced in cells. By irradiating cells in the presence of high concentrations of nontoxic cryoprotectants such as dimethyl sulfoxide (DMSO) or glycerol (which are also commonly used hydroxyl radical scavengers), it is possible to obtain an experimental estimate of the proportions of these contributions.⁹

Current experimental model systems for the direct effect inevitably take steps to attenuate the otherwise overwhelmingly large contribution of the indirect effect. These involve dehydration or cryogenic temperatures (or both) in order to remove its

source or limit the diffusion of the solvent radicals responsible for it.^{10–13} Such conditions may poorly model subsequent reactions of DNA radical species with water and oxygen, both of which are known to play important roles in the production of stable end products.² In an effort to overcome some of these limitations, we have developed a model system for examining the direct effect at room temperature in dilute aqueous solution. It involves using cationic peptide ligands to aggregate plasmid targets into a nanoparticulate condensate. This system provides a means with which we have been able to model the radiation chemistry of DNA with amino acid residues.¹⁴ This represents an important step, because in cellular chromatin there is an intimate association of DNA with binding proteins such as histones.¹⁵

Plasmid DNA molecules in these condensates exhibit a strongly attenuated reactivity with the hydroxyl radical, which is the species largely responsible for the indirect effect of ionizing radiation.² Therefore we wished to quantify the hydroxyl radical yield in these condensates. DNA binding ligands have found application in measuring the hydroxyl radical yield produced by the radioactive decay of Auger emitting isotopes.¹⁶ Thus we have explored the possibility of extending the technique to condensed plasmid DNA targets. The hydroxyl radical yield in these nonhomogeneous systems can be quantified by applying an existing fluorescent assay.¹⁷

In general, the detection of so-called reactive oxygen species using fluorescent means is subject to numerous artifacts.¹⁸ However, these concerns do not typically apply to the hydroxyl radical. Hydroxylation of aromatic rings is a characteristic feature

Received: June 2, 2011

Revised: June 26, 2011

Published: July 08, 2011

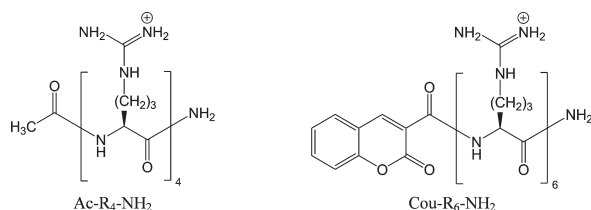


Figure 1. Chemical structures of the two oligoarginine ligands Ac-R₄-NH₂ and Cou-R₆-NH₂.

of the chemical reactivity of the hydroxyl radical,¹⁹ which can be exploited to develop specific and sensitive assays for it.^{20–23} For example, in the cases where the aromatic compound is a benzoate, a coumarin, a quinolone, or a phenoxazinone, at least one of the hydroxylated products is highly fluorescent.²⁴ These are respectively a salicylate, an umbelliferone, a hydroxyquinolone, or a resorufin. For various reasons, most of these systems are unsuitable as hydroxyl radical probes. The excitation wavelengths for salicylates are inconveniently located in the UV region and overlap extensively with absorption by the DNA bases (and numerous other cellular constituents). An additional chromatographic separation step is therefore frequently necessary. The yield of fluorescent hydroxylated quinolones is very poor. Phenoxazinones are not generally available with the exception of Actinomycin D, a well-studied DNA binding drug.²⁵ However, it too is hydroxylated to a fluorescent product in poor yield, presumably because its very large cyclic peptide side chains provide numerous alternative reaction sites. Although other methods also exist,²⁶ these considerations account for the popularity of the coumarin (sometimes described as a chromenone) group as a hydroxyl radical probe.^{16,17,24} In addition, simple umbelliferones,^{27–29} the fluorescent products derived from the coumarin system, have both excitation and emission wavelength ranges in common with the DAPI and Hoechst dyes frequently used in fluorescence microscopy. Therefore instrumentation for their detection tends to be widely available.

By incorporating the coumarin group into a cationic peptide that binds very strongly to DNA and then using an additional less strongly bound unlabeled ligand, it is in principle possible to produce a solution of labeled plasmid nanoparticles³⁰ in which the concentration of unbound label is very small. We have characterized the conditions under which the formation of the fluorescent product reflects the hydroxyl radical yield within the nanoparticulate plasmid condensate and not in the bulk of the solution.

MATERIALS AND METHODS

Biochemicals. A commercial (Invitrogen, Carlsbad, CA) sample of plasmid pUC18 (length 2686 bp) was grown in bacterial culture on a milligram scale, isolated, and purified as described previously.³¹ The ligands *N*-acetyl-tetra-arginine amide (Ac-R₄-NH₂) and *N*-(coumarin-3-carboxyl)-hexa-arginine amide (Cou-R₆-NH₂) were obtained commercially (Biosynthesis, Lewisville, TX). Their chemical structures are depicted in Figure 1.

Plasmid Solutions. The assays described below were applied to aqueous solutions containing sodium phosphate (5×10^{-3} mol L⁻¹, pH 7.0), sodium perchlorate (zero, or 1×10^{-3} to 0.5 mol L⁻¹), plasmid pUC18 ($10 \mu\text{g mL}^{-1}$, equivalent to a base pair concentration of 1.5×10^{-5} mol L⁻¹), one or both of the ligands Ac-R₄-NH₂ or Cou-R₆-NH₂ (zero, or 1×10^{-6} to

1×10^{-4} mol L⁻¹), and glycerol (zero, 1×10^{-4} to 0.1 mol L⁻¹). Because the physical properties of solutions containing aggregates of plasmid and ligand are known to change for some minutes after mixing,³² the plasmid was the last component added to these mixtures, and a period of 30 min was allowed to elapse before analysis or irradiation.

Static Light Scattering. The intensity of static light scattering (SLS) at a nominal angle of 90° was quantified (200 μL aliquot) using a model F-7000 fluorescence spectrometer (Hitachi, Pleasanton, CA) with both the excitation (optical path length 10 mm) and emission (optical path length 2 mm) monochromators set to 400 nm (bandwidth in both cases 5 nm). Neither the DNA bases nor the coumarin group of Cou-R₆-NH₂ exhibit any significant absorption at this wavelength.

Sedimentation. The concentration of the plasmid remaining in the supernatant after centrifugation at $15\,000 \times g$ for 10 min (200 μL aliquot) was determined from a measurement of the absorbance at 245 nm (optical path length 10 mm, bandwidth <2 nm) of the supernatant (120 μL) using a model DU-800 spectrometer (Beckman Coulter, Fullerton, CA). Although the maximum absorption of DNA is located at 260 nm, a wavelength of 245 nm was used here for its detection because, under the experimental conditions, the contribution of the coumarin chromophore of Cou-R₆-NH₂ to absorption at 245 nm is negligible. After centrifugation under the same conditions, the concentration of the ligand Cou-R₆-NH₂ remaining in solution was determined from the absorbance at 340 nm (optical path length 10 mm, bandwidth <2 nm), at which wavelength the plasmid makes a negligible contribution.

Gamma Irradiation. The effect of gamma irradiation (662 keV photon) on aqueous solutions or suspensions containing ligand(s) and plasmid pUC18 was examined by using a cesium-137 (400 Ci, 1.5×10^{13} Bq) isotopic source in a GammaCell-1000 instrument (J. L. Shepherd, San Fernando, CA). The absorbed dose rate of 276 rad min^{-1} ($4.6 \times 10^{-2} \text{ Gy s}^{-1}$) was determined using the Fricke method.¹⁹

Agarose Gel Electrophoresis. After gamma irradiation, aliquots (16 μL) of solutions containing plasmid DNA and ligand were treated with a loading buffer (8 μL) containing sucrose (30%), sodium perchlorate (usually 0.6 mol L^{-1} , but in some cases for low ionic strength solutions containing Cou-R₆-NH₂ it was necessary to increase this to 1.5 mol L^{-1}), and bromophenol blue (1 mg mL^{-1}). The resulting solutions were loaded into the wells of an agarose gel (1.2%) in the TBE buffer system ($8.9 \times 10^{-2} \text{ mol L}^{-1}$ Tris, $8.9 \times 10^{-2} \text{ mol L}^{-1}$ boric acid, $1 \times 10^{-3} \text{ mol L}^{-1}$ EDTA) and then subjected to electrophoresis (current 20 mA, electric field 1.8 V cm^{-1}) for 13 h. The fraction of the plasmid in the supercoiled form was quantified by digital video imaging of ethidium fluorescence using a GelDoc-XR instrument (Bio-Rad, Hercules, CA).

Yield of DNA Single Strand Breaks. The D_0 is defined as the absorbed dose of γ radiation required to decrease by a factor of e the fraction of the plasmid in the supercoiled form, which contains no strand breaks. This dose is numerically equal to the reciprocal of the slope m of a straight line fitted to a semilogarithmic yield dose plot. Assuming a Poisson distribution of DNA single strand breaks (SSBs), the D_0 dose produces a mean of one SSB per plasmid, so that the concentration of the SSB product is equal to that of the plasmid. During irradiation this concentration is equal to $1.5 \times 10^{-5} \text{ mol L}^{-1}$ base pairs, which is equivalent to $1.5 \times 10^{-5}/2686 = 5.6 \times 10^{-9} \text{ mol L}^{-1}$ in terms of the macromolecular plasmid (since pUC18 is 2686 base pairs in

length). The radiation chemical yield (or G-value) of SSB events is calculated by dividing this concentration by the value of D_0 .

Nucleic Acid Thermal Denaturation. It was not feasible to employ this assay with plasmid pUC18 because its melting temperature was higher than that achievable with the instrument. Therefore we used instead the sodium salt of double stranded poly(deoxyadenylic-thymidylic) acid (Sigma, St. Louis, MO, abbreviated as poly(dAT)₂). Its thermal denaturation (800 μ L sample volume) was examined under conditions otherwise identical to those described above for the plasmid (5×10^{-3} mol L⁻¹ sodium phosphate, pH 7.0, no added sodium perchlorate, 1.5×10^{-5} mol L⁻¹ base pair concentration), and assayed from the increase in absorbance at 245 nm (see above for the reason this wavelength was used, optical path length 10 mm, bandwidth <2 nm). The extrapolated temperature dependencies of the absorbance of the fully double-stranded (low temperature) and fully single-stranded (high temperature) forms were removed by subtraction.^{33,34} These measurements were made with a model DU-800 spectrophotometer (Beckman Coulter, Fullerton, CA) containing a temperature regulation accessory.

Fluorescence Spectroscopy. To quantify ethidium fluorescence, we used a solution of the same composition and volume used for thermal denaturation but with the additional presence of 1×10^{-6} mol L⁻¹ ethidium bromide. The intensity of the fluorescence due to ethidium was determined using a model F-7000 fluorescence spectrometer (Hitachi, Pleasanton, CA) by using an excitation wavelength of 490 nm (bandwidth 10 nm, optical path length 10 mm) and an emission wavelength of 590 nm (bandwidth 10 nm, optical path length 4 mm).

To quantify the formation of its fluorescent product, a solution containing the ligand Cou-R₆-NH₂ (3×10^{-6} mol L⁻¹) was gamma irradiated in aqueous solution containing sodium phosphate (5×10^{-3} mol L⁻¹, pH 7.0) and glycerol (zero, or 1×10^{-4} to 0.1 mol L⁻¹). After irradiation, an aliquot (200 μ L) was diluted with an equal volume of a solution containing sodium carbonate (0.1 mol L⁻¹, pH 10.3) and sodium perchlorate (1 mol L⁻¹). The intensity of the fluorescence (excitation wavelength 400 nm, bandwidth 10 nm, optical path length 10 mm; emission wavelength 440 nm, bandwidth 10 nm, optical path length 4 mm) was compared with that of a spectroscopically calibrated solution of 7-hydroxycoumarin-3-carboxylate (excitation 380 nm, emission 450 nm, bandwidths and optical path lengths as above). Its extinction coefficient under these conditions was taken as $\epsilon = 3.2 \times 10^4$ L mol⁻¹ cm⁻¹.²⁷ In both cases, a horizontally oriented plane polarizing filter was placed in the excitation light path to attenuate the intensities of the elastically scattered (Rayleigh) and inelastically scattered (Raman) light.³⁵

Atomic Force Microscopy. Samples were prepared by depositing an aliquot (5 μ L) of a solution containing sodium phosphate (5×10^{-3} mol L⁻¹, pH 7.0), plasmid pUC18 (10 μ g mL⁻¹), and either Ac-R₄-NH₂ (3×10^{-5} mol L⁻¹) or Cou-R₆-NH₂ (8×10^{-6} mol L⁻¹) onto a surface of freshly cleaved mica (1 cm \times 1 cm) followed by air drying. No additional cation was employed.

Topographic (in which intensity corresponds to height) images were collected using a multimode 8 instrument (Bruker, Santa Barbara, CA) using the peak force tapping mode and ScanAsyst air probes (force constant 0.3 N m⁻¹, resonant frequency 70 kHz). The instrument employs an automated proprietary feedback parameter optimization. The peak force tapping mode modulates the vertical piezo elements at ca. 2 kHz at each pixel of the image. The peak interaction force is used as

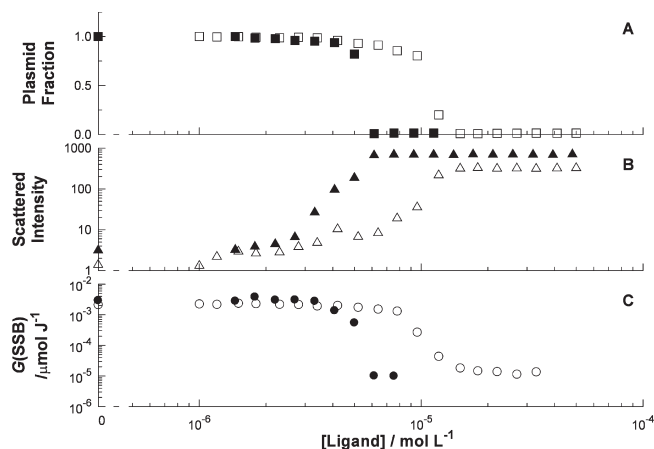


Figure 2. Fraction of plasmid pUC18 remaining in solution after centrifugation (panel A, square symbols), scattering intensity of light at 400 nm by pUC18 (panel B, triangle symbols), and SSB yield in pUC18 after gamma irradiation (panel C, circle symbols) as a function of the concentration of either the ligand Ac-R₄-NH₂ (open symbols) or Cou-R₆-NH₂ (filled symbols).

the feedback signal to estimate the topography. The scan speed was 1 line of 512 pixels per second. Minor image processing was used for the purposes of removing horizontal scanning artifacts and improving contrast.

RESULTS

Structures of the Ligands. We used a combination of two different ligands (Figure 1) to examine the hydroxyl radical yield in close proximity to DNA in a nanoparticle plasmid condensate. The hexa-arginine probe ligand bearing the coumarin label (Cou-R₆-NH₂, charge $Z = +6$) was intentionally more highly positively charged than the unlabeled auxiliary tetra-arginine ligand (Ac-R₄-NH₂, $Z = +4$). Ligands bearing higher charges are well-known to exhibit higher binding constants to DNA substrates.³⁶ In aqueous solution, DNA condensation with cationic ligands requires extensive neutralization of its negative charge.³⁷ In practical terms this implies at least a slight excess of the ligand. Under such conditions, the inevitable presence of even a small fraction of any unbound labeled ligand would be expected to respond to the very large yields of the hydroxyl radical in the bulk of the solution instead of the significantly smaller yields expected in the highly scavenged microenvironment of a DNA condensate.^{14,38} Therefore we have employed a limiting concentration of a strongly binding labeled ligand (Cou-R₆-NH₂) in the presence of an excess of a more weakly binding unlabeled ligand (Ac-R₄-NH₂).

Ligand Plasmid Interaction. We examined the effects on the plasmid in aqueous solution of the two ligands individually and jointly. The effects of the concentration of the ligands Ac-R₄-NH₂ and Cou-R₆-NH₂ on the plasmid were examined using sedimentation, SLS, and sensitivity to gamma irradiation (Figure 2). SLS was monitored at 400 nm, a wavelength intentionally chosen to be longer than the absorption bands of the DNA bases in the plasmid and also of the coumarin group in Cou-R₆-NH₂. Both ligands produced large increases (over 2 orders of magnitude) in light scattering over a narrow concentration range of about 2-fold. The midpoint of these increases is located at ca. 1×10^{-5} mol L⁻¹ Ac-R₄-NH₂ and 5×10^{-6} mol L⁻¹ Cou-R₆-NH₂. We also observed a large increase in the sedimentation rate of the

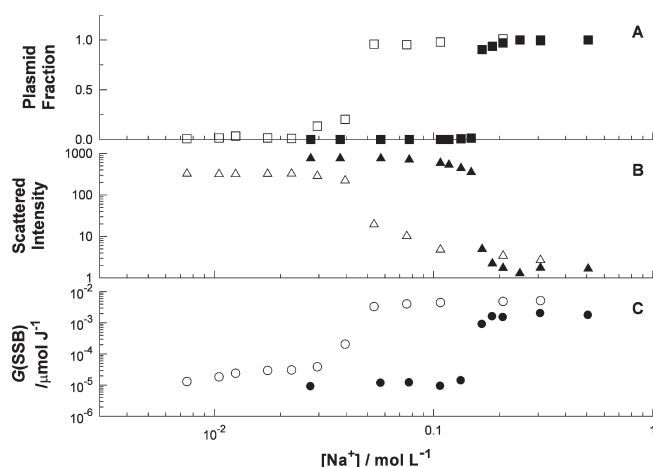


Figure 3. Fraction of plasmid pUC18 remaining in solution after centrifugation (panel A, square symbols), scattering intensity of light at 400 nm by pUC18 (panel B, triangle symbols), and SSB yield in pUC18 after gamma irradiation (panel C, circle symbols) in the presence either of $3 \times 10^{-5} \text{ mol L}^{-1}$ Ac-R₄-NH₂ (open symbols) or of $8 \times 10^{-6} \text{ mol L}^{-1}$ Cou-R₆-NH₂ (filled symbols) as a function of the sodium ion concentration.

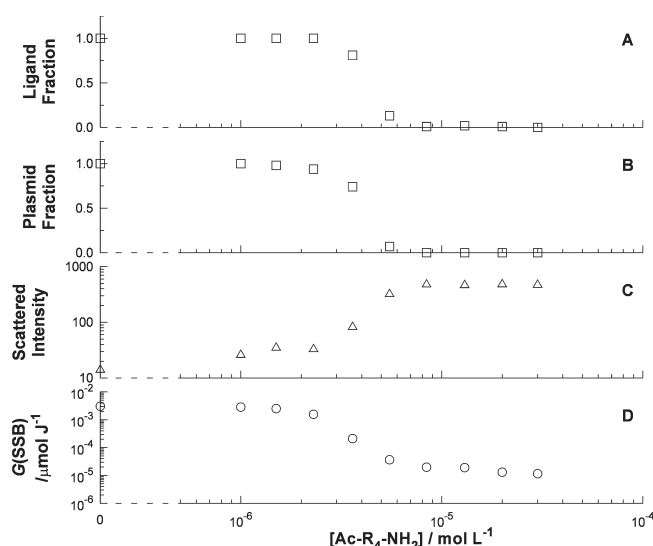


Figure 4. Fraction of the ligand Cou-R₆-NH₂ remaining in solution after centrifugation (panel A, square symbol), fraction of plasmid pUC18 remaining in solution after centrifugation (panel B, square symbol), scattering intensity of light at 400 nm by pUC18 (panel C, triangle symbol), and SSB yield in pUC18 after gamma irradiation (panel D, circle symbol) in the presence of $3 \times 10^{-6} \text{ mol L}^{-1}$ Cou-R₆-NH₂ as a function of the concentration of the additional ligand Ac-R₄-NH₂.

plasmid. The largest light scattering signals corresponded with an undetectable (<ca. 1%, given the sensitivity of the spectrometer) amount of the plasmid remaining in solution after centrifugation. These effects were also associated with a large decrease in the SSB yield produced in the plasmid by gamma irradiation. Similar effects have been reported with penta-arginine and with oligolysines.^{14,30}

We also examined the effect of sodium ion concentration on these three properties (Figure 3). We selected ligand concentrations of either $3 \times 10^{-5} \text{ mol L}^{-1}$ Ac-R₄-NH₂ or $8 \times 10^{-6} \text{ mol}$

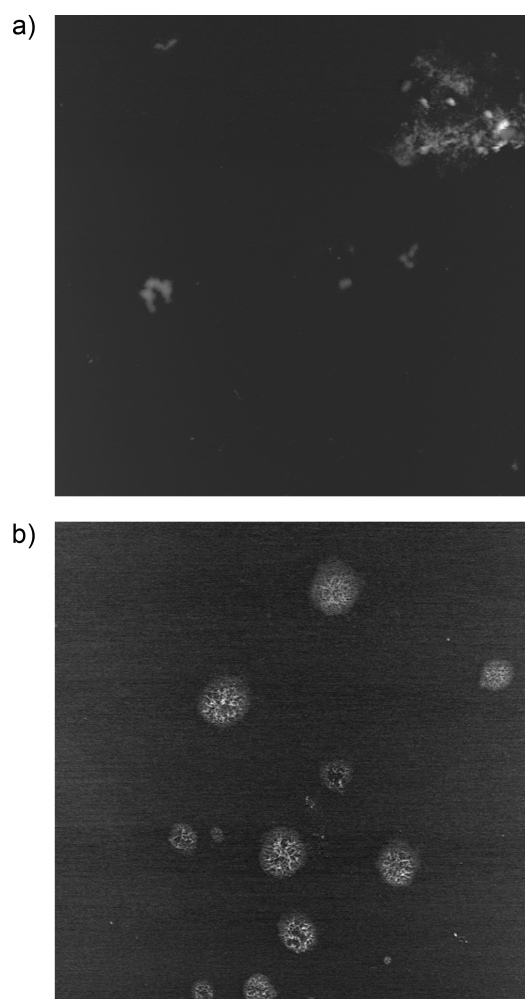


Figure 5. Atomic force microscopic images of plasmid DNA in the presence of either Ac-R₄-NH₂ (panel A) or Cou-R₆-NH₂ (panel B). The horizontal dimensions of both images are $10 \mu\text{m} \times 10 \mu\text{m}$. The vertical scale is 10 nm.

L^{-1} Cou-R₆-NH₂, in both cases high enough to bring about rapid sedimentation, a large SLS signal, and an extensive radioprotection (see Figure 2). Increasing ionic strength was able to restore the behavior of the plasmid to that observed in the absence of any added ligand. A gradual change in properties was evident for Ac-R₄-NH₂ with a midpoint at a sodium ion concentration of about $4 \times 10^{-2} \text{ mol L}^{-1}$. By contrast, the ligand Cou-R₆-NH₂ required a significantly larger sodium ion concentration of 0.15 mol L^{-1} , and the changes in properties were very sharply defined. Again, similar effects have been observed previously.¹⁴

We also examined the simultaneous presence of both ligands. The concentration of Ac-R₄-NH₂ was increased from zero to $3 \times 10^{-5} \text{ mol L}^{-1}$ while Cou-R₆-NH₂ was also present at a constant concentration of $3 \times 10^{-6} \text{ mol L}^{-1}$ (Figure 4). The same increases in sedimentation, SLS, and radioprotection were observed, but with the midpoints located at the lower Ac-R₄-NH₂ concentration of ca. $5 \times 10^{-6} \text{ mol L}^{-1}$. In addition, it was observed that the presence of $3 \times 10^{-5} \text{ mol L}^{-1}$ Ac-R₄-NH₂ (a 10-fold excess) was not able to displace Cou-R₆-NH₂ from the plasmid, since the latter ligand was not detectable in solution under conditions that resulted in sedimentation of all of the plasmid. The limit of detection for Cou-R₆-NH₂ depends on the

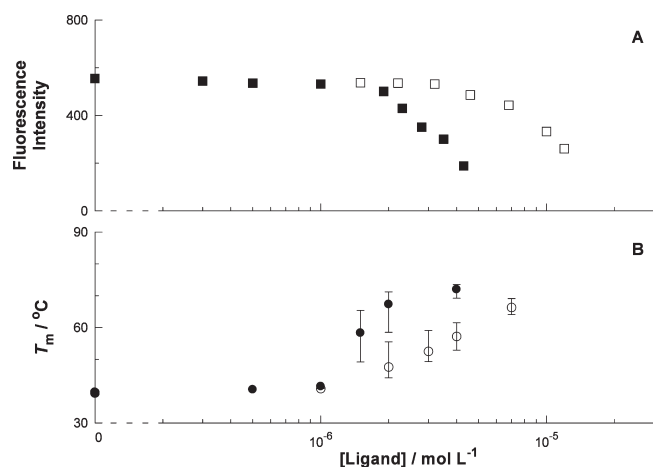


Figure 6. Effect of either the ligand Ac-R₄-NH₂ (open symbol) or Cou-R₆-NH₂ (closed symbol) on ethidium fluorescence intensity (panel A, square symbol) and on thermal denaturation (panel B, circle symbol) of the artificial homopolymer poly(dAT)₂. The vertical scale in panel A is arbitrary. In panel B, the location of the circular symbols represents 50% denaturation, while the error bars represent the 20th and 80th percentiles. Error bars smaller than the symbols are not shown.

extinction coefficient of its UV absorption, and is on the order of 1% of the ligand.

An increase in sedimentation rate and in SLS is suggestive of aggregation of the plasmid into larger particles.³⁷ The concentration of Cou-R₆-NH₂ required to achieve these effects is well-defined in Figure 2 as just over $5 \times 10^{-6} \text{ mol L}^{-1}$. For a $Z = +6$ species, this corresponds to $3 \times 10^{-5} \text{ mol L}^{-1}$ positively charged arginine residues. Assuming a mean relative molecular mass of 325 per nucleotide residue, the plasmid concentration of $10 \mu\text{g mL}^{-1}$ corresponds to a nucleotide residue concentration of $10 \times 10^{-3} / 325 = 3.1 \times 10^{-5} \text{ mol L}^{-1}$, in good agreement with the ligand concentration. Particles having dimensions on the order of $1 \mu\text{m}$ were detected in atomic force microscopy images of condensates produced with either $3 \times 10^{-5} \text{ mol L}^{-1}$ Ac-R₄-NH₂ or $8 \times 10^{-6} \text{ mol L}^{-1}$ Cou-R₆-NH₂ (Figure 5). Note, however, that these images are of dried samples, and it is doubtful that they are representative of the sizes of aggregates present in solution.

We also examined the interaction of the ligands with a nucleic acid using two assays that are, in principle, able to detect smaller extents of binding than those that produce large effects in sedimentation and elastic scattering. These were (1) a binding competition with a fluorescent DNA binding ligand and (2) the thermal denaturation of the nucleic acid (Figure 6). For this purpose, we used the artificial homopolymer poly(dAT)₂, whose strand separation is far more easily detected than is the case with the plasmid.⁴⁰ At concentrations too low to produce detectable changes in sedimentation, SLS, or radioprotection, the presence of the ligands slightly decreased the fluorescence due to bound ethidium and produced a unequivocal increase of 25–30 °C in the temperature at which strand dissociation took place, with Cou-R₆-NH₂ having an effect at lower concentrations (ca. $1.5 \times 10^{-6} \text{ mol L}^{-1}$) than Ac-R₄-NH₂ (ca. $4 \times 10^{-6} \text{ mol L}^{-1}$). In the absence of any added ligand, this melting process took place over a very narrow temperature range. Modest ligand concentrations produced large increases in this range, but the range was observed to decrease again at larger ligand concentrations.

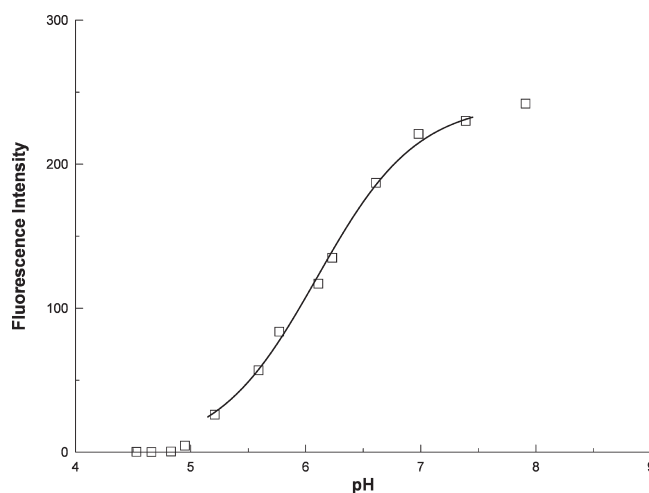


Figure 7. Fluorescent intensity of gamma irradiated Cou-R₆-NH₂ as a function of pH. The data are fitted with the Henderson equation assuming $\text{pK}_a = 6.1$. The vertical scale is arbitrary.

Similar effects on melting range have been reported for polyamine ligands⁴⁰ and interpreted in terms of a stochastic binding model.⁴¹

Formation and Yield of Fluorescent Product. When an aqueous solution of $3 \times 10^{-6} \text{ mol L}^{-1}$ Cou-R₆-NH₂ and $1 \times 10^{-4} \text{ mol L}^{-1}$ glycerol was subjected to a 10 Gy dose of gamma irradiation, a fluorescent species was detectable with excitation and emission maxima at 400 and 450 nm, respectively. The locations of the absorption and emission bands of this fluorescent product derived from Cou-R₆-NH₂ are similar to those of the phenolate form of coumarin-3-carboxylic acid (excitation 380 nm, emission 440 nm, not shown). They are also in good agreement with a report of an umbelliferone derivative of a polyamine.¹⁶

We also examined the pH dependence of this radiation-induced fluorescence intensity (Figure 7). The irradiation was at pH 7.0, and the pH was adjusted afterward. The fluorescence was weak under acidic conditions, but became more intense with increasing pH. The fluorophore is characterized by an acid dissociation constant of ca. 6.1. This value is significantly lower than that for 4-methylumbelliferone ($\text{pK}_a = 7.8^{42}$), but such a difference is consistent with the highly positively charged ($Z = +6$) nature of the ligand.

The yield in which this fluorescent product was formed from the hydroxyl radical was estimated by quantifying the fluorescence produced after gamma irradiation of a solution containing only Cou-R₆-NH₂ and phosphate buffer components. The fluorophore produced by irradiation of the ligand was assumed to be characterized by a brightness (the product of the extinction coefficient ϵ at the excitation maximum and the quantum yield ϕ) identical to that of the phenolate forms of authentic umbelliferones. For example, by using the values of $\epsilon = 3.2 \times 10^4 \text{ L mol}^{-1} \text{ cm}^{-1}$ and $\phi = 0.7$ for 7-hydroxycoumarin-3-carboxylate and 4-methylumbelliferone, respectively,^{27–29} it was then possible to convert fluorescence intensity into concentration.

In the absence of any added glycerol, the slope of the resulting yield dose plot was found to be $1.40 \times 10^{-2} \mu\text{mol J}^{-1}$. This value represents the radiation chemical yield (conventionally referred to as the G -value) of the fluorescent product when its precursor

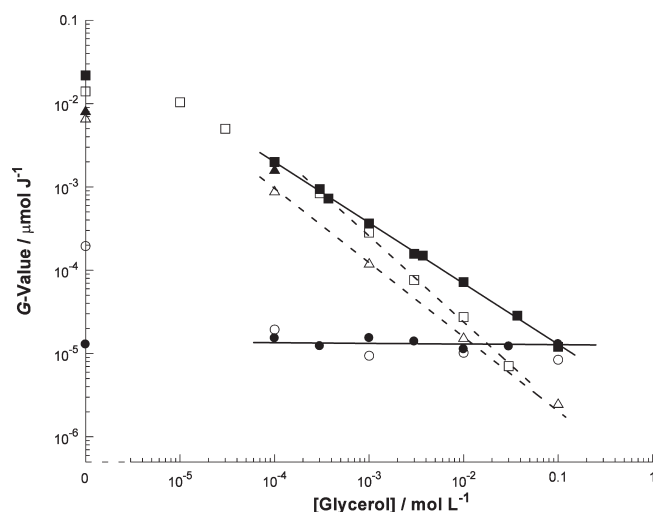


Figure 8. Dependence on glycerol concentration of the radiation chemical yields of SSB formation in pUC18 plasmid DNA (closed symbols) and of the formation of the 7-hydroxylated derivative of the ligand Cou-R₆-NH₂ (open symbols) in aqueous solution. The plasmid ($10 \mu\text{g mL}^{-1}$) and Cou-R₆-NH₂ ($3 \times 10^{-6} \text{ mol L}^{-1}$) were irradiated together along with Ac-R₄-NH₂ ($3 \times 10^{-5} \text{ mol L}^{-1}$) and in the absence of sodium perchlorate (circle symbols); together with Ac-R₄-NH₂ ($3 \times 10^{-5} \text{ mol L}^{-1}$) but in the presence of 0.3 mol L^{-1} sodium perchlorate (triangle symbols); or separately (square symbols). Four of the data sets are fitted with least mean square straight lines of the form $y = cx^m$. The values of the slopes m are 0.0 (filled circle), -0.7 (filled square), -0.9 (open triangle), and -1.0 (open square).

is essentially the only species in solution that reacts with the hydroxyl radical. Dividing this value by the yield of the hydroxyl radical under the irradiation conditions provides the fraction of hydroxyl radicals that react with Cou-R₆-NH₂ to produce a fluorescent product. In these dilute solutions, the value of $G(\cdot\text{OH})$ may be taken as ca. $0.28 \mu\text{mol J}^{-1}$.⁴³ Therefore the yield of the fluorescent product derived from Cou-R₆-NH₂ is estimated to be $1.40 \times 10^{-2} / 0.28 = 5.0\%$ of the hydroxyl radical yield. This value is consistent with that of 4.7% for the formation of 7-hydroxycoumarin-3-carboxylic acid from coumarin-3-carboxylic acid.²⁴

To test the ability of the ligand Cou-R₆-NH₂ to act as a fluorescent probe for the hydroxyl radical, it was gamma irradiated in aqueous solution under three different conditions. First, the ligand Cou-R₆-NH₂ ($3 \times 10^{-6} \text{ mol L}^{-1}$) was irradiated in the absence of any added plasmid DNA, but in the presence of glycerol. Second, the ligand Cou-R₆-NH₂ ($3 \times 10^{-6} \text{ mol L}^{-1}$) was irradiated in the presence of Ac-R₄-NH₂ ($3 \times 10^{-5} \text{ mol L}^{-1}$) and pUC18 plasmid DNA ($10 \mu\text{g mL}^{-1}$), but also in the presence of 0.3 mol L^{-1} sodium perchlorate. This salt concentration was chosen to prevent the large changes in sedimentation and elastic light scattering from taking place (see Figure 3). Third, the ligand Cou-R₆-NH₂ ($3 \times 10^{-6} \text{ mol L}^{-1}$) was irradiated in the presence of Ac-R₄-NH₂ ($3 \times 10^{-5} \text{ mol L}^{-1}$) and pUC18 plasmid DNA ($10 \mu\text{g mL}^{-1}$), but in the absence of any sodium perchlorate. This third set of conditions was chosen to permit the large changes in sedimentation and light scattering to occur. The radiation chemical yields of the fluorescent product (estimated as above) derived from Cou-R₆-NH₂ and also of the SSB yield in plasmid pUC18 were determined under these three sets of conditions. All are plotted in Figure 8. For comparative

purposes, Figure 8 also includes SSB yields observed in pUC18 after irradiation in the absence of any added ligand but in the presence of glycerol.

In the absence of any glycerol, the fluorescent product is formed from Cou-R₆-NH₂ with a yield of $1.4 \times 10^{-2} \mu\text{mol J}^{-1}$ (see above). The presence during irradiation of $10^{-5} \text{ mol L}^{-1}$ glycerol slightly attenuates this yield to $1.0 \times 10^{-2} \mu\text{mol J}^{-1}$. Larger concentrations of glycerol produce a larger attenuation, and the yield decreases to about $1 \times 10^{-5} \mu\text{mol J}^{-1}$ (over 3 orders of magnitude) at 0.1 mol L^{-1} glycerol. The limiting slope of the straight line fitted to these data is $m = -1.0$. A generally similar behavior is observed in the competition between the plasmid and glycerol, where an SSB is the detected product. The SSB yield decreases from ca. $2 \times 10^{-2} \mu\text{mol J}^{-1}$ (no glycerol) to $10^{-5} \mu\text{mol J}^{-1}$ (0.1 mol L^{-1} glycerol), again by about 3 orders of magnitude. However, the SSB yield shows a weaker dependence on the glycerol concentration, with a limiting slope of $m = -0.7$. Similar observations have been reported previously.⁴⁴

When both ligands and the plasmid are present in solution and irradiated in the additional presence of sodium perchlorate, the formation of the fluorescent product from Cou-R₆-NH₂ and of the SSB product in the plasmid are very similar to the yields observed when the ligand or the plasmid are irradiated separately. At low glycerol concentrations ($< \text{ca. } 10^{-2} \text{ mol L}^{-1}$), the presence of Ac-R₄-NH₂ and the plasmid results in a small (ca. 2 fold) decrease in the yield of the fluorescent product from Cou-R₆-NH₂. At higher glycerol concentrations, this difference vanishes. The limiting slope of the glycerol concentration dependence is $m = -0.9$. The SSB yields observed in the plasmid are 2–3 fold lower in the absence of glycerol, but become indistinguishable at glycerol concentrations greater than $10^{-4} \text{ mol L}^{-1}$.

When both ligands and the plasmid are present in solution, and irradiated in the absence of sodium perchlorate, the radio-protective effects associated with the large changes in sedimentation and light scattering (Figure 2) again become apparent. The SSB yield in the plasmid is independent of the glycerol concentration, and remains at ca. $1 \times 10^{-5} \mu\text{mol J}^{-1}$. The yield of the fluorescent product formed from Cou-R₆-NH₂ is $2 \times 10^{-4} \mu\text{mol J}^{-1}$ in the absence of glycerol. This yield decreases to ca. $2 \times 10^{-5} \mu\text{mol J}^{-1}$ at $10^{-4} \text{ mol L}^{-1}$ glycerol, but exhibits only a 2-fold further decrease at higher glycerol concentrations.

DISCUSSION

Ligand Plasmid Interaction. Micromolar concentrations of the ligand Cou-R₆-NH₂ are observed to decrease ethidium fluorescence presumably by displacing it from the plasmid⁴⁵ and also to produce large increases in the melting temperature (Figure 6). Similar effects are observed with Ac-R₄-NH₂, although requiring ca. 2-fold higher ligand concentrations. These results are in agreement and suggest that both ligands bind to poly(dAT)₂,^{33,34,40} with Cou-R₆-NH₂ binding more strongly than Ac-R₄-NH₂. We assume that this observation for poly(dAT)₂ is also valid for plasmid pUC18.

Both the sedimentation and SLS assays reflect an increase in particle size and strongly suggest that if present at sufficient concentration, the ligands are able to produce aggregates of multiple plasmids, a process conventionally referred to as DNA condensation.³⁷ This is supported by the observation of objects with dimensions in the micrometer range using atomic force microscopy (Figure 5). The use of polyarginine in gene transfer

depends on the formation of DNA aggregates.³⁹ The changes in physical properties correlate very closely with a decrease in the SSB yield by over two (at 10^{-4} mol L⁻¹ glycerol, Figures 2 and 8) or 3 orders of magnitude (in the absence of glycerol, Figure 8). There is a significantly poorer correlation of the SSB yield with the effect on thermal denaturation. Therefore it is not ligand binding *per se*, but its promotion of plasmid aggregation that is responsible for radioprotection of the plasmid.³⁰ Therefore, when in the condensed form, the plasmid target is highly resistant to reaction with the hydroxyl radical, a product of the gamma radiolysis of water. The more highly charged ligand Cou-R₆-NH₂ is able to produce this aggregation at a lower concentration (6×10^{-6} mol L⁻¹ Cou-R₆-NH₂ against 1.5×10^{-5} mol L⁻¹ Ac-R₄-NH₂), and it requires a much larger ionic strength to reverse this ability (0.15 mol L⁻¹ Na⁺ for Cou-R₆-NH₂ against 4×10^{-2} mol L⁻¹ Na⁺ for Ac-R₄-NH₂). The stabilizing effect of the ligands on thermal denaturation of poly(dAT)₂ implies that they bind preferentially with double stranded nucleic acids,³³ and that the binding of Cou-R₆-NH₂ is stronger than that of Ac-R₄-NH₂.

These results all suggest that the ligand Cou-R₆-NH₂ binds more strongly to DNA than Ac-R₄-NH₂, and they are consistent with the inability of excess Ac-R₄-NH₂ to displace Cou-R₆-NH₂ from plasmid DNA. This general behavior is expected from the charge difference between the two ligands, and agrees with previous observations with oligolysines.^{36,46}

Quantitative data is available in the literature for the binding constants of oligoarginines to DNA, and for their ionic strength dependencies.⁴⁶ These were obtained by fluorescence quenching of a single tryptophan residue located in the oligoarginine. Under our experimental conditions, at a sodium ion concentration of 7.5×10^{-3} mol L⁻¹ (the contribution made by the phosphate buffer system in the absence of any added sodium perchlorate), the binding constant for RWR₄-NH₂ (with charge, $Z = +6$) is about 10^3 fold larger than that for RWR₂-NH₂ ($Z = +4$). Our data for the ligand concentration dependencies of sedimentation, SLS, and radioprotection (Figure 2), for thermal denaturation (Figure 6), and for the ionic strength effects (Figure 3) are entirely consistent with the assumption that these values are representative of the two ligands Cou-R₆-NH₂ ($Z = +6$) and Ac-R₄-NH₂ ($Z = +4$) that we have used. We argue that the presence of a limiting concentration of Cou-R₆-NH₂ and the presence of an excess of Ac-R₄-NH₂ produces a nanoparticulate suspension of the plasmid condensate in which it may be assumed that the vast majority of the coumarin label is bound to the plasmid. This hypothesis is further examined below.

Nature and Yield of the Fluorescent Product. The fluorescent product formed by gamma irradiation of an aqueous solution of Cou-R₆-NH₂ displays an excitation maximum at 400 nm and an emission maximum at 450 nm. These wavelengths are similar to those of authentic 7-hydroxylated coumarins.^{28,29} They are also in good agreement with those reported for polyamine derivatives of 7-hydroxycoumarins.¹⁶ At $pK_a = 6.1$, the dissociation constant of the product is significantly lower than that of the phenolic group of 4-methylumbelliferone ($pK_a = 7.8$).⁴² However, a higher acidity is entirely consistent with the strongly positively charged nature of a hexa-arginine species. Therefore we assume that the fluorescence observed after irradiation of Cou-R₆-NH₂ is due to hydroxylation of the coumarin group at the 7-position to form the umbelliferone fluorophore.^{16,17,24}

The estimate of the yield of 7-hydroxylation per hydroxyl radical of 5.0% for Cou-R₆-NH₂ compares with 4.7% for

coumarin-3-carboxylate.²⁴ The similarity of these yields implies that the hydroxyl radical shows very little reactivity with the peptide region in Cou-R₆-NH₂. This is in agreement with the low reactivity of arginine with the hydroxyl radical.⁴⁷

Behavior of Cou-R₆-NH₂ as a Hydroxyl Radical Probe. The results plotted in Figure 8 permit an evaluation of the ligand Cou-R₆-NH₂ as a probe for the hydroxyl radical. When the only competition for the hydroxyl radical is between Cou-R₆-NH₂ and glycerol, the decrease in the yield of the fluorescent product with increasing glycerol concentration can be understood in terms of simple competition kinetics ($m = -1.0$ in Figure 8). The competition for the hydroxyl radical between the plasmid and glycerol ($m = -0.7$) is more complex, and indicates that the rate coefficient for the reaction of the plasmid with the hydroxyl radical increases with increasing glycerol concentration. This nonhomogeneous kinetic effect may be qualitatively understood in terms of a rapid depletion of hydroxyl radicals in close proximity to the macromolecular plasmid, with the observed rate coefficient strongly depending upon the diffusion of further hydroxyl radicals down the resulting concentration gradient.^{48,49} The diffusion distance decreases with increasing glycerol concentration, producing a corresponding increase in the experimentally observed rate coefficient.⁴⁴ The existence of this effect appears to be important in understanding the reactivity of the ligand Cou-R₆-NH₂, because of its tendency to associate with the plasmid.

Under conditions where both Cou-R₆-NH₂ and Ac-R₄-NH₂ and the plasmid are all present in solution, but the binding of the ligands to the plasmid is inhibited by a high ionic strength, the SSB yield in the plasmid is largely unaffected by the ligands. The SSB yield is determined almost entirely by competition with glycerol.³¹ This behavior is understandable since, at their low concentrations, the ligands make very little contribution to scavenging the hydroxyl radical in the bulk of the solution. The ligands are largely dissociated from the plasmid, so they also poorly compete for the hydroxyl radical in its vicinity. There is some evidence for partial plasmid binding of Cou-R₆-NH₂, however, because the glycerol attenuation of the yield of the fluorescent product (characterized by $m = -0.9$) exhibits some deviation from simple competition kinetics ($m = -1.0$) in the direction of a less negative slope. This result would be expected for a species for which a significant fraction is bound to the plasmid.

When the plasmid is irradiated in the condensed form, the SSB yield is independent of the presence of glycerol and remains constant at a level about 3 orders of magnitude lower than when essentially all the hydroxyl radicals formed by irradiation are able to react with the plasmid. The same is not true, however, of the ligand Cou-R₆-NH₂. The yield of its fluorescent product decreases by ca. 10-fold when the glycerol concentration is increased from zero to 10^{-4} mol L⁻¹, although further increases in the glycerol concentration have very little effect, producing an additional attenuation of only 2-fold. This effect is indicative of a small fraction of unbound Cou-R₆-NH₂ present in solution. While unbound Cou-R₆-NH₂ is undetectable in Figure 4, the sensitivity of the spectrophotometric assay is necessarily limited by its extinction coefficient. Unbound Cou-R₆-NH₂ is accessible to hydroxyl radicals in the bulk of the solution, although its low concentration results in an unfavorable competition against even low glycerol concentrations. Therefore as long as precautions are taken to address the issue of the small unbound fraction of the labeled ligand, it offers a

means to quantify the hydroxyl radical yield in the close proximity of the substrate to which it is bound.¹⁶

Existing experimental methods used to examine DNA damage by the direct effect of ionizing radiation do so by an extensive attenuation of the indirect effect. This is achieved by severe conditions involving dehydration and/or cryogenic temperatures.^{10–13} There is a concern that these systems may poorly model important reactions of radical species with water and oxygen. It is possible that the use of nanoparticulate plasmid condensates may offer an alternative means with which to examine the direct effect. The use of a polyamine-coumarin conjugate as a hydroxyl radical probe in the neighborhood of DNA has been reported in conjunction with Auger emission.¹⁶ We argue that the use of a commercially available peptide ligand may offer a simpler alternative.

CONCLUSION

When both ligands and the plasmid are present in solution at a low ionic strength, ligand binding is sufficiently extensive under the experimental conditions to aggregate multiple plasmids into larger condensates. In this form, the plasmid is extensively protected against the bulk of the solution. In the absence of any additional glycerol, the SSB yield is attenuated by 3 orders of magnitude. The enormous size of this attenuation of the yield of the indirect effect, produced by a total ligand concentration ($3 \times 10^{-6} \text{ mol L}^{-1} \text{ Cou-R}_6\text{-NH}_2 + 3 \times 10^{-5} \text{ mol L}^{-1} \text{ Ac-R}_4\text{-NH}_2 = 3.3 \times 10^{-5} \text{ mol L}^{-1}$ ligand) of the same order as the concentration of the plasmid ($1.5 \times 10^{-5} \text{ mol L}^{-1}$ base pairs), provides a convenient model system with which to study the direct effect in dilute aqueous solution at room or physiological temperatures. In addition, the use of the labeled ligand Cou-R₆-NH₂ provides a convenient means with which to quantify the hydroxyl radical yield within a few nanometers of the DNA to which it is tightly bound.

AUTHOR INFORMATION

Corresponding Author

*E-mail: jmilligan@ucsd.edu. Phone: 858-534-4919. Fax: 858-534-0265.

ACKNOWLEDGMENT

This work was supported by PHS Grant CA46295.

REFERENCES

- (1) Sage, E.; Harrison, L. *Mutat. Res.* **2011**, 711, 123.
- (2) von Sonntag, C. *Free Radical Induced DNA Damage and Its Repair. A Chemical Perspective*; Springer: New York, 2006.
- (3) Becker, D.; Adhikary, A.; Sevilla, M. In *Recent Trends in Radiation Chemistry*; Wishart, J. F., Rao, B. S. M., Eds.; World Scientific Publishing Co. Pte. Ltd.: Singapore, 2010; p 509.
- (4) Von Sonntag, C. In *Recent Trends in Radiation Chemistry*; Wishart, J. F., Rao, B. S. M., Eds.; World Scientific Publishing Co. Pte. Ltd.: Singapore, 2010; p 543.
- (5) Bernhard, W. A.; Close, D. M. In *Charged Particle and Photon Interactions with Matter*; Mozumder, A., Hatano, Y., Eds.; Marcel Dekker: New York, 2003; p 471.
- (6) ESR *Studies of Radiation Damage to DNA and Related Biomolecules*; Sevilla, M. D., Becker, D., Eds.; The Royal Society of Chemistry: Cambridge, U.K., 2004; Vol. 19, p 243.
- (7) Sevilla, M. D.; Bernhard, W. A. In *Radiation Chemistry: From Basics to Applications in Material and Life Sciences*; Spothem-Maurizot, M., Mostafavi, M., Douki, T., Belloni, J., Eds.; EDP Sciences: Les Ulis, France, 2008; p 191.
- (8) Daban, J.-R. *Biochem. Cell. Biol.* **2003**, 81, 91.
- (9) Chapman, J. D.; Reuvers, A. P.; Borsa, J.; Greenstock, C. L. *Radiat. Res.* **1973**, 56, 291.
- (10) Sharma, K. K.; Milligan, J. R.; Bernhard, W. A. *Radiat. Res.* **2008**, 170, 156.
- (11) Adhikary, A.; Khanduri, D.; Sevilla, M. D. *J. Am. Chem. Soc.* **2009**, 131, 8614.
- (12) Yokoya, A.; Cuniffe, S. M. T.; Watanabe, R.; Kobayashi, K.; O'Neill, P. *Radiat. Res.* **2009**, 172, 296.
- (13) Swarts, S. G.; Becker, D.; Sevilla, M.; Wheeler, K. T. *Radiat. Res.* **1996**, 145, 304.
- (14) Ly, A.; Bullick, S.; Won, J.-H.; Milligan, J. R. *Int. J. Radiat. Biol.* **2006**, 82, 421.
- (15) van Holde, K.; Zlatanova, J. *Semin. Cell. Dev. Biol.* **2007**, 18, 651.
- (16) Singh, A.; Yang, Y.; Adelstein, S. J.; Kassiss, A. I. *Int. J. Radiat. Biol.* **2008**, 84, 1001.
- (17) Collins, A. K.; Makrigiorgos, G. M.; Svensson, G. K. *Med. Phys.* **1994**, 21, 1741.
- (18) Wardman, P. *Free Radical Biol. Med.* **2007**, 43, 995.
- (19) Spinks, J. W. T.; Woods, R. J. *An Introduction to Radiation Chemistry*, 3rd ed.; Wiley: New York, 1990.
- (20) Matthews, R. W. *Radiat. Res.* **1980**, 83, 27.
- (21) Freinbichler, W.; Bianchi, L.; Colvicchi, M. A.; Ballini, C.; Tipton, K. F.; Linert, W.; Della Corte, L. *J. Inorg. Biochem.* **2008**, 102, 1329.
- (22) Villeneuve, L.; Alberti, L.; Steghens, J.-P.; Lancelin, J.-M.; Mestas, J.-L. *Ultrason. Sonochem.* **2009**, 16, 339.
- (23) Maeyama, T.; Yamashita, S.; Baldacchino, G.; Taguchi, M.; Kimura, A.; Murakami, T.; Katsumura, Y. *Radiat. Phys. Chem.* **2011**, 80, 535.
- (24) Newton, G. L.; Milligan, J. R. *Radiat. Phys. Chem.* **2006**, 75, 473.
- (25) Biver, T.; Venturini, M.; Jares-Erijman, E. A.; Jovin, T. M.; Secco, F. *Biochemistry* **2009**, 48, 173.
- (26) Tai, C.; Gu, X.; Zou, H.; Guo, Q. *Talanta* **2002**, 58, 661.
- (27) Adamczyk, M.; Cornwell, M.; Huff, J.; Rege, S.; Rao, T. V. S. *Bioorg. Med. Chem. Lett.* **1997**, 7, 1985.
- (28) Sherman, W. R.; Stanfield, E. F. *Biochem. J.* **1967**, 102, 905.
- (29) Malet, C.; Planas, A. *Biochemistry* **1997**, 36, 13838.
- (30) Tsoi, M.; Do, T. T.; Tang, V.; Aguilera, J. A.; Perry, C. C.; Milligan, J. R. *Biophys. Chem.* **2010**, 147, 104.
- (31) Milligan, J. R.; Aguilera, J. A.; Ward, J. F. *Radiat. Res.* **1993**, 133, 151.
- (32) Vilfan, I. D.; Conwell, C. C.; Sarkar, T.; Hud, N. V. *Biochemistry* **2006**, 45, 8174.
- (33) Spink, C. H.; Wellman, S. E. *Methods Enzymol.* **2001**, 340, 193.
- (34) Mergny, J.-L.; LaCroix, L. *Oligonucleotides* **2003**, 13, 515.
- (35) Lackowicz, J. R. *Principles of Fluorescence Spectroscopy*, 3rd ed.; Springer: New York, 2006.
- (36) Nayvelt, I.; Thomas, T.; Thomas, T. J. *Biomacromolecules* **2007**, 8, 477.
- (37) Newton, G. L.; Aguilera, J. A.; Ward, J. F.; Fahey, R. C. *Radiat. Res.* **1996**, 145, 776.
- (38) Bloomfield, V. A. *Curr. Opin. Struct. Biol.* **1996**, 6, 334.
- (39) Emi, N.; Kidoaki, S.; Yoshikawa, K.; Saito, H. *Biochem. Biophys. Res. Commun.* **1997**, 231, 421.
- (40) Plum, G. E.; Bloomfield, V. A. *Biopolymers* **1990**, 29, 13.
- (41) Ambjörnsson, T.; Banik, S. K.; Krichevsky, O.; Metzler, R. *Biophys. J.* **2007**, 92, 2674.
- (42) Graber, M. L.; DiLillo, D. C.; Friedman, B. L.; Pastoriza-Munoz, E. *Anal. Biochem.* **1986**, 156, 202.
- (43) Pimblott, S. M.; LaVerne, J. A. *Radiat. Res.* **1998**, 150, 159.
- (44) Milligan, J. R.; Wu, C. C.; Ng, J. Y.; Aguilera, J. A.; Ward, J. F. *Radiat. Res.* **1996**, 146, 510.
- (45) Stootman, F. H.; Fisher, D. M.; Rodger, A.; Aldrich-Wright, J. R. *Analyst* **2006**, 131, 1145.

- (46) Mascotti, D. P.; Lohman, T. M. *Biochemistry* **1997**, *36*, 7272.
- (47) Buxton, G. V.; Greenstock, C. L.; Helman, W. P.; Ross, A. B. *J. Phys. Chem. Ref. Data* **1988**, *17*, 513.
- (48) Mark, F.; Becker, U.; Herak, J. N.; Schulte-Frohlinde, D. *Radiat. Environ. Biophys.* **1989**, *28*, 81.
- (49) Bluett, V. M.; Green, N. J. *J. Phys. Chem. A* **2006**, *110*, 6112.